THE RUN II DØ CALORIMETER : ELECTRONICS UPGRADE AND ITS PERFORMANCE

NIRMALYA PARUA
State University of New York, Stony Brook, USA
E-mail: parua@fnal.gov

(for the DØ Collaboration)

The front-end electronics of the DØ calorimeter has undergone a complete redesign to operate successfully with the shorter bunch spacing time at the RunII of the Fermilab Tevatron. After the successful installation of the new electronics, first results of the commissioning, the calibration and the performance of the calorimeter will be presented.

1. Introduction

The DØ detector performed extremely well during Run I (1992-1996) at the Fermilab Tevatron. The calorimeter is a key component of the DØ detector and has provided excellent accuracy and resolution in measuring the position and energy of electrons, photons, jets and inferring the presence of neutrinos in events. The discovery of top quark and subsequent measurement of its mass and production cross section relied heavily on the calorimeter. Also calorimeter has been instrumental in the precision measurement of the mass of the W boson; the search for new particles and anomalous couplings; verification of quantum chromodynamics; and important measurements of electroweak physics. During RunI Tevatron delivered to both CDF and DØ, about 125 pb^{-1} of integrated luminosity with peak instantaneous luminosity of $1.6 \times 10.^{31}$ cm $^{-2}$ s^{-1}. The accelerator has undergone major upgrade, in order to deliver the larger luminosities needed to study low cross section and high p_T processes such as top, Higgs, W/Z and physics beyond the standard model. The goal of this upgrade is to deliver at the first phase of RunII, 20 times more luminosity compared to RunI. Two main components of the accelerator upgrade are the addition of the Main Injector and the anti-proton recycler. The center of mass energy of collision has also been raised from 1.8 TeV to 1.96 TeV. The Tevatron has been operational since March 2001. The higher instantaneous luminosity requires a reduction in the bunch spacing time from the RunI value of 3.5 μs to

396 ns for the first phase and then to 132 ns for the second phase of RunII. The upgrade of the DØ detector is designed to enhance its capabilities from RunI and to accommodate the new beam structure in its readout. In the following we will briefly overview major upgrades of the DØ detector and then discuss the upgrades for calorimeter in more details.

2. Overview of the DØ Detector Upgrade

Figure 1 depicts the overview of the upgraded DØ detector. The tracking system is completely replaced with a Silicon Micro-strip Tracker (SMT) and a Central Fiber Tracker (CFT) with scintillating fiber readout. The entire tracking system is contained inside a 2.8m superconducting solenoid that produces a 2 T magnetic field. To compensate for the energy loss in the solenoid, central and forward preshower detectors are introduced. Both these detectors consist of scintillator strips fitted with wavelength shifting fiber readout. Although the uranium liquid-Argon calorimeter remained untouched in RunII, most of the readout system was replaced to handle the smaller bunch spacing time. The Photo multiplier tubes used for the scintillator based Inter Cryostat Detector (ICD) were relocated to a region of lower magnetic field. The RunII muon system includes scintillator based detectors used to provide a fast trigger. Also, in the forward muon system the Proportional Drift tubes were replaced with planes of plastic Mini Drift Tubes (MDTs). Massive shielding is used to reduce backgrounds originating from scattered protons and antiprotons. To deal with the high event rate, the trigger system needed a full replacement with a 3-tier system and fast pipelined front-ends. The newly designed first stage (L1 trigger) incorporates the signals from the scintillator detectors, tracking and the calorimeter detectors. L1 trigger reduces the input rate of 1.7 MHz to 10 kHz. L1 trigger decision time is 4.2 μs and it is essentially deadtimeless. The L2 trigger consist of dedicated processors that must make the decisions in 100 μs and further reduce the rate to 1 kHz. The third stage trigger (L3) consist of a farm of commercial processors that utilize fully digitized information to reduce the L3 accept rate to 50Hz.

3. Inter Cryostat Detector

In the intermediate region of the calorimeter ($1.1 \leq |\eta| \leq 1.4$) energy measurements are degraded due to un-instrumented regions and the rapidly changing material profile. The Inter Cryostat detector (ICD) restores the energy resolution of jets in this region and the missing transverse energy ($\not\!\!E_T$) of an event by providing additional sampling. The ICD detector consist of 384 scintillator tiles with wavelength shifting fibers (WLS) read out using photomultiplier

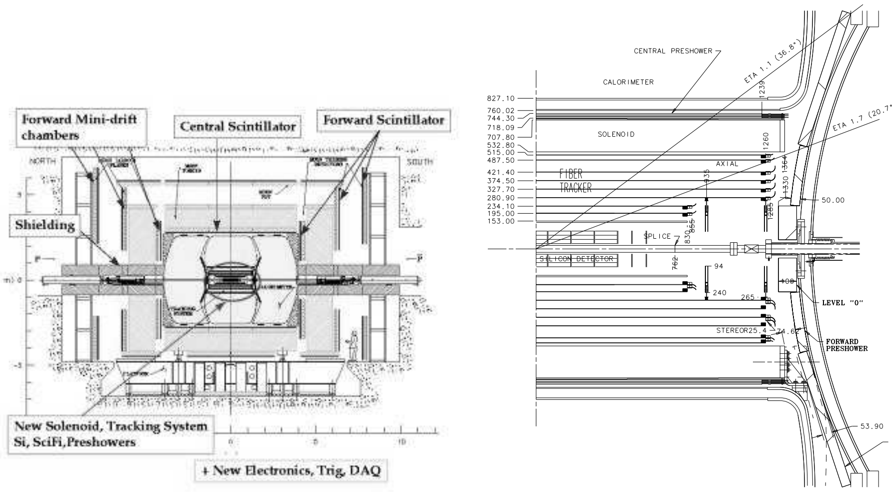

Figure 1. (Left) Side view of the upgraded DØ detector. (Right) side view of one half of the tracking system.

tubes. The tile signals are transported to a region of low magnetic field by 5-6 m long clear fiber waveguides. The 384 tiles each cover a region of 0.1×0.1 in $\eta - \phi$ space and are grouped into two sets of 16 supertiles per end cap (EC).

4. Liquid Argon Calorimeter

A detailed description of the DØ calorimeter can be found elsewhere [1]. In this section we briefly summarize important features of the calorimeter. The DØ calorimeter uses liquid argon as the active medium and with depleted uranium plates as the primary absorber material except in the the outer layers where stainless steel and copper plates are used. The schematic design of the calorimeter is shown in Fig. 2. The central calorimeter (CC) covers roughly a region in $|\eta| \leq 1$ and the two end calorimeters (EC) extend the coverage up-to $|\eta| \approx 4$. The Inter-cryostat Detector (ICD) covers the overlap region between CC and EC. The calorimeter is modular and is finely segmented in the transverse and longitudinal directions of the shower. Three distinct types of modules are used in the calorimeter: a finely segmented electromagnetic section with 2mm uranium absorber plates; a fine hadronic section (FH) with thicker uranium absorber plates than EM section; and a coarse hadronic section (CH) with thick copper and stainless steel plates. Each module consists of a stack of interleaved absorber plates and signal boards as shown in the Fig. 2. The absorber plates are separated from signal boards by a liquid argon gap of

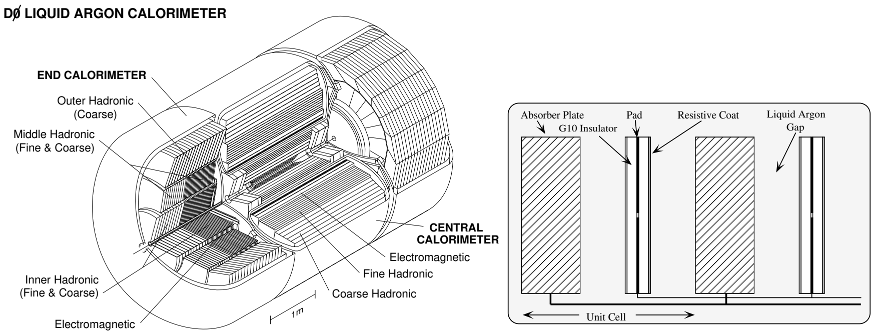

Figure 2. The DØ Calorimeter.

2.3 mm. Signal boards are constructed by laminating a copper pad with two 0.5 mm thick pieces of G10. The outer surface of these boards are coated with resistive epoxy. An electric field is applied by grounding the metal absorber plate and by biasing the resistive coat to 2kV. The electron drift time across the gap is $\approx 430ns$. This sets the time scale for signal charge collection. Signals from several pads at approximately the same η and ϕ are ganged together in depth to form a readout cell. The readout layers are arranged into pseudo-projective towers.

4.1. *Upgraded Calorimeter Electronics*

The goal in replacing the calorimeter electronics was to maintain the same overall noise performance achieved in RunI. The noise is the sum of electronic, uranium and pile-up contributions. To achieve this goal it was necessary to optimize the relative noise contributions and to add analog storage device on which to store the calorimeter signals until a L1 trigger decision could be made. This required a new strategy for baseline subtraction. A schematic diagram of the RunII calorimeter readout is shown in the Fig 3. The signal from each of 55,000 cells is brought to the feed-through port (a sealed interface between the inside and outside of the cryostat) on a 30Ω co-axial cable. The original 115 Ω twist and flat cables from the feed-through port to the preamplifiers ($\sim$ 5-7 m) were replaced with 30 Ω coaxial cables to provide: impedance matching to the preamplifiers; faster charge collection; individual channel timing equalization. About 55000 individual hybrid charge sensitive preamplifiers were built for the calorimeter signals. The new design has lower noise and improved drive capability. Two additional driver stages were added to drive the single ended 115 Ω cable to the shaping circuitry, the base line subtracter (BLS), and to allow for the option of differential outputs. The preamplifier

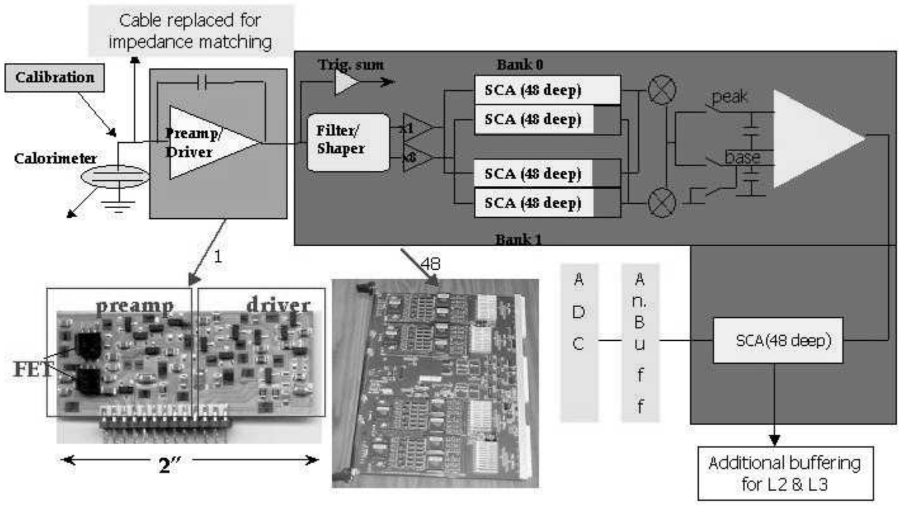

Figure 3. Readout chain of the calorimeter in RunII

uses two jFET's (2sk369) in parallel to reduce the electronic noise (at the cost of additional power consumption). This reduces the noise level by a factor of $1/\sqrt{2}$ and partly compensates for the increase in noise level arising from the reduction in shaping time (which scales as $1/\sqrt{shaping\ time}$). Fourteen different species of preamplifiers are used in Run II to compensate for the effect of varying detector capacitances. Forty-eight preamplifier hybrids are socket mounted on a single preamplifier mother board that connects to the backplane of the preamplifier box. Each box houses 96 preamplifier motherboards and are powered by low noise 2kW commercial switching power supplies. Calibration pulses are injected through 0.1 % precision resistors. The preamplifier output is brought to the BLS unit through 115Ω twist and flat cables of length 25 m. BLS unit is located in the platform below the detector. The output pulse of the preamplifier has rise time of 430 ns and decay time of 15 μs. In order to reduce pile-up effects the preamplifier output is differentiated with a time constant of 250 ns. The shaped output is sampled at its peak at about 320 ns, and the voltage signal is stored in an analog pipeline called the switched capacitor array (SCA). The SCAs are 48 channels deep, and can thus hold the signals until a L1 trigger decision can be made 4.2 μs (32 samples taken every 132 ns) later. The SCAs are not designed for simultaneous read and write operations. Two SCAs are used for the same channel so that one SCA can be readout while the other is being written. At a L1 trigger rate of 10KHz this provides for a deadtimeless operation. The SCA has a 12 bit precision. In order to achieve the required 15 bit dynamic range, shaped signals are passed through two different gain paths ($\times 1$ and $\times 8$). Both are simultaneously sampled and stored into two parallel SCAs. So a total of 4 L1 analog buffers are used for every channel. In order to remove slowly varying offsets, and pileup of events from neighboring bunch crossings, samples taken 396 ns earlier are subtracted from the sample taken at trigger time and the subtracted signal is stored in a fifth SCA of same depth as the L1 pipeline, where it awaits a L2 trigger decision. After the L2 trigger accept is received, the signal is readout from the appropriate depth in the L2 SCA for digitization by the ADC. The ADC is a successive approximation digitizer and has been retained from RunI. The ADC has 12 bit of dynamic range but a low and high gain path ($\times 1$ and $\times 8$) maintains the 15 bit dynamic range. The calorimeter L1 trigger uses a fast trigger pickoff signal obtained by hard differentiation of the preamplifier output by a shaper hybrid located on the BLS unit. Trigger towers are formed by summing over all channels with $\Delta\eta \times \Delta\phi$ of 0.2×0.2. The summation is done in two stages on the BLS unit, the second stage is also used to drive the signal to the L1 trigger system. Coordination between the trigger framework and the calorimeter readout is done by the timing and the control system. It receives trigger, accelerator and clock information through the serial command link (SCL) and oversees that the appropriate depth in the pipeline is readout at every trigger level.

4.2. *Commissioning of the Calorimeter Electronics*

The installation and commissioning of new electronics was nearly complete at the time of the conference only awaiting the full trigger coverage. At the time of the conference the L1 calorimeter trigger coverage was complete up to $|\eta| \leq 0.8$. At present it is extended up to $|\eta| \leq 2.4$. The rest of the calorimeter trigger is expected to be finished shortly. We have measured the liquid argon impurity to be less than 0.15 ppm [2] which is less than the 0.5 ppm specification. At the beginning of the commissioning we checked continuity of the cables inside the cryostat and from the feed-through port to the preamplifier by injecting a step pulse and measuring the reflected pulse from the calorimeter cells. The reflected pulse shape can be modeled by using appropriate detector capacitances and cable impedances. Using this method we have found less than 0.05 % of the cables have problems that can not be repaired. These bad cables are randomly distributed, and thus have minimal impact on the calorimeter data. We have also debugged the entire readout chain by reading out the means of pedestals and the noise for every channel. The response of every channel to the injected calibration pulses has been checked. After removal of bad channels we are left with $\leq 0.05\%$ bad channels. These bad channels are also randomly distributed over the entire detector and are being suppressed during data taking. We have measured the distribution of correlation coefficients for pairs of channels. From the deviation of this distribution from the expected Gaussian distribution we have estimated that the correlated noise is ≤ 0.05 ADC counts. A correlated noise study is underway to measure the effect on the calorimeter readout due to other detector systems (SMT and CFT). As mentioned earlier, the calorimeter signal is sampled in every 132 ns and stored in analog pipelines (SCAs). It is very important to study the variation of this stored signal at all depths in the pipeline. We have done detailed study to measure the variation. About 1 % of all SCA chips showed sizable variation and those have been replaced with good chips. We have also confirmed that we are sampling the shaped calorimeter signal at its peak. This was done by taking 3 samples in an event (averaged over many events), with the nominal peak sample taken at the point as defined by the trigger, a second sample is taken at 132 ns earlier and a third one 132 ns later. The nominal sampling position with respect to the peak of the shaped signal can be accurately determined from the ratio of these samples when compared to a spice [3] model fit to the signal. Using this method we have determined that the channel-to-channel variation of the nominal sampling time is less than 10 ns. This implies less than 0.1% variation in the peak sampled value due to timing differences. A preliminary calibration study shows excellent linearity for calorimeter energy deposits greater than 1 GeV (the non-linearity is found to be $< 0.3\%$) [4]. For smaller energies the non-linearity is non-negligible, but is corrected by using a simple parametrization.

5. Physics Studies

We have started several physics analysis using calorimeter data. Preliminary results on W boson and Z boson production and their subsequent decay to electronic channels, W decay width etc. will be presented in the ICHEP conference. In Fig 4 preliminary plots of inclusive jet p_T spectrum and dijet mass spectrum is shown.

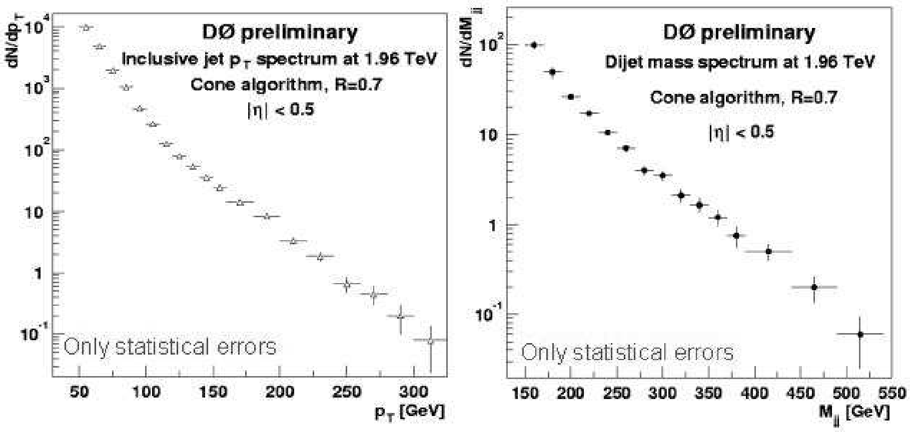

Figure 4. Inclusive jet p_T spectrum (left) and Dijet mass spectrum (right)

6. Outlook

We have recently finished commissioning most of the new calorimeter electronics. The remaining part of the trigger readout is expected to be done soon. The new calorimeter electronics is performing well. Benchmark physics processes using the calorimeter are being studied. Preliminary results are encouraging. In the near future we will be studying the calibration and jet energy scale in more detail.

Acknowledgments

Thanks to my DØ colleagues for doing the hard work that brought the detector to its present state. Also, their help in preparing the manuscript is highly appreciated. Thanks to the organizers for arranging a very enjoyable conference.

References

1. R. D. Schamberger, The DØ Calorimeter Performance and Calibration, in: Proc. fifth Calorimetry in High Energy Physics (ed. H. Gordon and D. Rueger, Upton, NY, September 1994), 39-50, (World Scientific, 1995). DØ Collaboration, S. Abachi *et al.*, Nucl. Instrum. Methods Phys. Res. **A 338**, 185 (1994).
2. A. Besson, Proceedings in this conference.
3. www.psspice.com
4. U. Bassler, Proceedings in this conference.